Epilepsia. Author manuscript; available in PMC 2013 October 07.

Published in final edited form as:

Epilepsia. 2009 April ; 50(4): 617–628. doi:10.1111/j.1528-1167.2008.01784.x.

Effect of sleep stage on interictal high-frequency oscillations recorded from depth macroelectrodes in patients with focal epilepsy

Andrew P. Bagshaw[*], **Julia Jacobs**[†], **Pierre LeVan**[†], **François Dubeau**[†], and **Jean Gotman**[†]

[*]School of Psychology, University of Birmingham, Birmingham, United Kingdom

[†]Montreal Neurological Institute and Hospital, McGill University, Montréal, Québec, Canada

Summary

Purpose—To investigate the effect of sleep stage on the properties of high-frequency oscillations (HFOs) recorded from depth macroelectrodes in patients with focal epilepsy.

Methods—Ten-minute epochs of wakefulness (W), stage 1–2 non-REM (N1-N2), stage 3 non-REM (N3) and REM sleep (R) were identified from stereo- electroencephalography (SEEG) data recorded at 2 kHz in nine patients. Rates of spikes, ripples (>80 Hz), and fast ripples (>250 Hz) were calculated, as were HFO durations, degree of spike–HFO overlap, HFO rates inside and outside of spikes, and inside and outside of the seizure-onset zone (SOZ).

Results—Ripples were observed in nine patients and fast ripples in eight. Spike rate was highest in N1-N2 in 5 of 9 patients, and in N3 in 4 of 9 patients, whereas ripple rate was highest in N1-N2 in 4 of 9 patients, in N3 in 4 of 9 patients, and in Win 1 of 9 patients. Fast ripple rate was highest in N1-N2 in 4 of 8 patients, and in N3 in 4 of 8 patients. HFO properties changed significantly with sleep stage, although the absolute effects were small. The difference in HFO rates inside and outside of the SOZ was highly significant ($p < 0.000001$) in all stages except for R and, for fast ripples, only marginally significant ($p = 0.018$) in W.

Conclusions—Rates of HFOs recorded from depth macroelectrodes are highest in non-REM sleep. HFO properties were similar in stages N1-N2 and N3, suggesting that accurate sleep staging is not necessary. The spatial specificity of HFO, particularly fast ripples, was affected by sleep stage, suggesting that recordings excluding REM sleep and wakefulness provide a more reliable indicator of the SOZ.

Keywords

Intracerebral EEG; High-frequency oscillations; Sleep

Address correspondence to Andrew P. Bagshaw, School of Psychology, University of Birmingham, Edgbaston, Birmingham B15 2TT, U.K. a.p.bagshaw@bham.ac.uk.

We confirm that we have read the Journal's position on issues involved in ethical publication and affirm that this report is consistent with those guidelines.

Disclosure: None of the authors has any conflict of interest to disclose.

Recent studies have reported the presence of high-frequency oscillations (HFOs) in the intracranial EEG (stereo-encephalography, SEEG) of patients with epilepsy, both in the ictal (Worrell et al., 2004; Jirsch et al., 2006) and interictal (Bragin et al., 1999a, 1999b, 2002; Staba et al., 2002, 2004; Urrestarazu et al., 2006; Staba 2007; Urrestarazu et al., 2007) periods. Oscillations above the gamma band (i.e., >80 Hz) are generally split into two categories according to their frequency: ripples (~100– 250 Hz) and fast ripples (>250 Hz). Ripples are considered to be a signature of both normal and pathologic brain processes (Draguhn et al., 2000; Engel et al., 2003), whereas fast ripples have been identified only in epileptogenic tissue in both patients and animal models of epilepsy (Bragin et al., 1999a, 1999b; Staba et al., 2002; Engel et al., 2003). As a consequence of this apparent link between HFOs and epileptogenicity, there is currently considerable interest in extending the usable bandwidth of clinical SEEG recordings to allow the analysis of HFOs. In particular, fast ripples have the potential to provide a more specific marker of the epileptogenic region, which in turn could lead to resections restricted more closely to the abnormal tissue.

Initial reports demonstrated that HFOs could be observed in the SEEG of patients with epilepsy using depth microelectrodes (Bragin et al., 1999a, 1999b, 2002). Microelectrodes consist of multiple microwires of approximately 40 μm diameter inserted through the middle of polyurethane multicontact SEEG probes (Bragin et al., 2002; Staba et al., 2007). Similar high-frequency events have also been reported using standard macroelectrodes (Jirsch et al., 2006; Urrestarazu et al., 2006, 2007), and oscillations up to 150 Hz have been recorded using foramen ovale electrodes (Clemens et al., 2007). The distinction between micro- and macroelectrodes is important, since the recording surface is several hundred times smaller with microelectrodes, and the size of the recording contact determines the extent of the neuronal populations that are sampled. In general the properties of HFOs that are recorded with the different electrode types have been similar (for example event rates and durations), although a recent study that used both microwires and macroelectrodes in the same patients found some differences, particularly in the frequency of HFOs (Worrell et al., 2008). Given the potentially different neuronal generators of the events, it is important that conclusions drawn from microelectrode recordings are verified when considering the use of macroelectrodes.

Macroelectrode recordings have the benefit that they are routinely used for clinical intracranial investigation, so modifications to allow the recording of HFOs are minimal, and involve primarily the filtering and sampling rate in the SEEG amplifiers. However, examination of SEEG data at a temporal resolution sufficiently high to allow identification of HFO events is extremely time-consuming, and the amount of data generated when recording with a suitable sampling rate is extremely large. Consequently, it is crucial that more specific knowledge is acquired about the rate of occurrence of HFO in relation to different behavioral states in order to maximize the probability of detecting the events of interest.

Previous work has indicated that the rate of HFOs recorded with microelectrodes (Staba et al., 2004) and foramen ovale electrodes (Clemens et al., 2007) is highest in non–rapid eye movement (non-REM) sleep, and this information has been used in some studies to focus the analysis specifically on slow-wave sleep, since it is a relatively easy stage of non-REM sleep

to detect (Urrestarazu et al., 2007; Jacobs et al., 2008; Worrell et al., 2008). However, the effect of sleep stage on HFO rates has not been addressed previously using depth macroelectrodes, and it has not been confirmed that the properties of HFOs recorded in different sleep stages remain constant. It is conceivable that sleep stage not only affects the rate of HFOs, but that HFO from different neuronal generators become evident in the different stages. For example, if the spatial specificity of fast ripples to epileptogenic regions changes as a function of sleep stage, it may be crucial to avoid certain periods when the spatial specificity is reduced, even if the event rate remains high. In addition, the relationship between the rate of HFO and the rate of interictal epileptiform discharges (IEDs) has not been investigated. It has been noted that HFOs are often associated with IEDs (Staba et al., 2004; Urrestarazu et al., 2006, 2007), and it is known that the rate of IED varies with sleep stage (see Gigli & Valente, 2000 for a review), but whether the relationship between HFO and IED remains stable as a function of sleep stage is not clear. This study examined these issues in a sample of patients with focal epilepsy who were undergoing presurgical evaluation.

Patients and Methods

Patient selection and recording methods

From a total of 37 patients who underwent electrode implantation at the Montreal Neurological Institute and Hospital between September 2004 and June 2007, patients were selected who had lesional localized epilepsies, electrode contacts in both spiking and nonspiking regions, one or two clear seizure-onset zones (SOZs), and contacts placed clearly within and outside SOZs. Following these criteria, 10 patients were identified. Of these, one was excluded from the current study because of the lack of electromyography (EMG)/ electro-oculography (EOG) electrodes, which were necessary for sleep staging. Consequently, nine patients were included in the current study.

All patients had complex partial seizures. In five patients, the seizure onset was located in the mesial temporal lobe structures. In the other four patients, seizure onset was neocortical: in temporal structures in two patients and other neocortical areas in two patients. In all but two patients, seizures originated from a single SOZ. In two patients, two different SOZs could be identified. Clinical details of the patients and electrode implantation sites are given in Table 1.

A combination of depth and cortical surface electrodes were implanted stereotactically according to clinical criteria using an image-guidance system (SSN Neuronavigation System, Mississauga, Canada). Electrodes were manufactured on site. A 10/1,000-in. wire of stainless steel was used as a central core and wrapped with a 3/1,000-in. steel wire. Each electrode had nine contacts, with the deepest contact (contact 1) consisting of the tip of the steel core stripped of insulation. Contact 1 had an uninsulated length of 1 mm, whereas all other contacts (2–9) were formed from stripped sections of the marginal wire that was tightly wound to create 0.5 mm long coils. The effective surface area for contact 1 was 0.80 mm^2 and 0.85- mm^2 for contacts 2 to 9.

Data were recorded using the Harmonie long-term monitoring system (Stellate, Montreal, Canada), with a low-pass filter of 500 Hz and a sampling rate of 2,000 Hz. In addition to the intracerebral electrodes, EOG and EMG were used to allow sleep staging. This study was approved by the research ethics committee of the Montreal Neurological Institute and Hospital, and all patients gave written informed consent.

Sleep staging and epoch selection

For each patient, 10 min epochs of wakefulness, stage 1–2 non-REM sleep, stage 3 non-REM sleep (slow-wave sleep) and REM sleep were identified in a two step process. The definitions of sleep stages were aligned as closely as possible to the recent American Academy of Sleep Medicine (AASM) Manual for the Scoring of Sleep and Associated Events (Iber et al., 2007), given the absence of scalp electrodes.

First, periods of 1–2 h were selected for each of the four stages. These periods were selected on the basis of two main criteria: that they were not within 2 h of a seizure, either before or after the epoch, and that the appropriate stage appeared to be present at some point. For this initial selection, the data were examined at a time resolution of 30 s per screen in Stellate Harmonie. Approximately five SEEG electrode contacts were displayed in addition to the EOG and EMG electrodes. These contacts were a subset of those chosen for the main analysis (see subsequent text).

For each of these large epochs, two SEEG electrode contacts and the EMG signal were subjected to spectral analysis (Fast Fourier Transform [FFT] with 4.096 s window length, subsequently averaged into 30 s epochs, activity from 30–100 Hz examined in the EMG channel). Using these data, 10 min epochs were selected, which demonstrated stable characteristics for each sleep stage:

- Wakefulness (Stage W according to Iber et al., 2007): EOG and EMG activity without artifacts from movement/chewing, etc., low delta activity on the SEEG.
- Stage N1-N2: low EMG, slow or no eye movements on the EOG, low delta activity on the SEEG.
- Stage N3 (slow-wave sleep): high delta activity on the SEEG with low EMG and no EOG activity.
- REM (Stage R): rapid eye movement EOG activity with minimal EMG, low delta activity on the SEEG.

Event selection

Given the large number of electrode contacts per patient and the duration required to identify HFOs manually, analysis was restricted to a limited selection of contacts. Electrode and contact selection was guided by the images of the neuronavigation system, and only those channels that were clearly located within the gray matter were chosen. Approximately equal numbers of spiking/nonspiking and SOZ/non-SOZ channels were selected per patient, leading to between 7 and 13 contacts per patient, depending on the number of lesions and SOZs. Table 1 gives details of the electrode contacts that were analyzed, and whether they were in the SOZ.

Data were viewed at the maximum time resolution, corresponding to approximately 0.6 s per screen (529 mm/s), and in a bipolar montage. The screen was split vertically into two sections, one of which showed the data high pass filtered at 80 Hz, and the other the data high pass filtered at 250 Hz (in both cases, a finite impulse response filter of order 63 was used). Ripples and fast ripples were identified visually and marked independently by specifying the start and end of the events. In both cases, oscillations were required to contain at least four consecutive peaks clearly visible above the background signal in the filtered data. The same 10-min epochs were marked for spikes by a separate observer examining the SEEG with standard display characteristics.

Data analysis

Several measures were calculated for each 10-min epoch to allow their variation to be assessed as a function of sleep stage. First, the rates of spikes, ripples, and fast ripples were calculated using custom code written in Matlab (MathWorks, Natick, MA, U.S.A.). Rates were calculated for each minute of the 10-min epoch, and the mean and standard deviation for all 1 min periods of the epoch were also calculated. The durations of ripples and fast ripples were investigated, as was the degree of overlap between ripples/fast ripples and spikes. In addition, the rates of ripples/fast ripples inside and outside of spikes, and inside and outside of the SOZ, were assessed across sleep stages. All of these measures were calculated for each patient and subsequently averaged across all patients. Statistical significance was assessed with one way analysis of variance (ANOVA), with post hoc pairwise comparisons performed using Tukey's HSD (honestly significant differences) test, corrected for multiple comparisons. Results were accepted as significant if $p < 0.05$. All figures give mean values plus and minus one standard error of the mean.

Results

All four sleep stages were identified in all patients with the exception of patient 4, for whom a sufficiently long period of REM sleep was not observed. Both ripples and fast ripples were observed in all but one patient, the exception being patient 4 for whom no fast ripples were identified. When HFOs were observed, they were generally seen in all sleep stages of a given patient, with the exception of patient 7 for whom no fast ripples were marked in either R or N3 sleep. Across all sleep stages and patients, 11,734 ripples and 4,771 fast ripples were identified from a total of 74 electrodes. Examples of ripples and fast ripples from various patients and sleep stages are shown in Fig. 1.

Figure 2 shows the rates of spikes, ripples, and fast ripples averaged over all patients and for each patient individually. The rate of fast ripples was highest in N1-N2 in 4 of 8 patients (one patient did not have any fast ripples), and in N3 in 4 of 8 patients. The rate of ripples was highest in N1-N2 in 4 of 9 patients, in N3 in 4 of 9 patients, and in W in 1 patient. For comparison, the rate of spikes was highest in N1-N2 in 5 of 9 patients, and in N3 in 4 of 9 patients. In general, both ripples and fast ripples had their maximal rate in the same sleep stage as the spikes. For example, for the four patients whose maximal rate of fast ripples was in N3, the rate of spikes was also highest in N3 (see Fig. 2).

These general observations were supported by the statistical analysis. Overall, there was no statistically significant difference in rate of fast ripples in N1-N2 and N3 sleep ($p = 0.81$), whereas all comparisons between N1-N2 or N3 and W or R were highly significant ($p < 0.000001$ for W vs. N1-N2, W vs. N3, R vs. N1-N2, and R vs. N3). There was no statistically significant difference between the rate of fast ripples in W and R ($p = 0.90$). For ripples, the rate in N3 was significantly higher than in N1-N2 ($p = 0.003$), comparisons between N1-N2 or N3 and W or R were highly statistically significant ($p < 0.000001$ for W vs. N1-N2, W vs. N3, R vs. N1-N2, and R vs. N3), and there was no statistically significant difference between the rates in W and R ($p = 0.95$).

Figure 3 shows the mean duration of ripples and fast ripples across all patients throughout sleep stages. Fast ripple durations varied significantly as a function of sleep stage, with an approximately linear increase as sleep stage varied through W-N1-N2-N3-R. All paired comparisons of fast ripple duration were significant, with the exception of that between N3 and R (W vs. N1-N2, $p = 0.003$;Wvs. N3, $p = 0.000001$; W vs. R, $p = 0.00003$; N1 vs. N2-N3, $p = 0.007$; N1-N2 vs. R, $p = 0.027$; N3 vs. R, $p = 0.42$). Differences in ripple duration as a function of sleep stage were also statistically significant for all paired comparisons ($p < 0.00001$ for the comparisons between W vs. N1-N2, W vs. N3, N1-N2 vs. N3, N1-N2 vs. R, and N3 vs. R; $p = 0.0004$ for W vs. R), with the highest mean ripple duration observed during N3. Although these paired comparisons demonstrated that ripple and fast ripple durations were affected by sleep stage, the absolute differences were relatively small. Fast ripple durations were particularly stable, ranging from a mean value during wakefulness of 28.9 ms to a mean value during R of 34.6 ms. The equivalent range for ripples was from 58.0 ms in W to 71.1 ms in N3.

Figure 4 shows the effect of sleep stage on the fraction of ripples and fast ripples, which overlapped with spikes. For fast ripples, the most significant differences were seen between N1-N2 vs. N3 ($p < 0.000001$) and N1-N2 vs. R ($p = 0.0006$). Other comparisons were either nonsignificant or marginally significant (W vs. N3, $p = 0.02$; W vs. R, $p = 0.02$; N3 vs. R, $p = 0.54$; W vs. N1-N2, $p = 0.85$). For ripples, all comparisons were significant except for that between N3 and R (W vs. N1-N2 and W vs. N3, $p < 0.000001$; N1-N2 vs. R, $p = 0.0003$; N1-N2 vs. N3, $p = 0.002$; W vs. R, $p = 0.04$; N3 vs. R, $p = 0.06$). Overall the values calculated for different sleep stages were highly consistent, with a similar proportion of HFO events overlapping with spikes. For example, the mean values for spike–fast ripple overlap for N1-N2 and N3 were 0.20 and 0.23, respectively (this comparison was statistically significant at $p < 0.000001$).

Examination of the rates of HFOs that were and were not coincident with spikes demonstrated similar patterns as a function of sleep stage (Fig. 5). Rates were maximal for both ripples and fast ripples in either N1-N2 or N3, irrespective of whether the events were coincident with a spike. Of note, there was no statistically significant difference between the rate of fast ripples coincident with spikes between stages N1-N2 and N3 ($p = 0.84$), but the rate outside of spikes was significantly higher in N3 than in N1-N2 ($p < 0.000001$).

Finally, to examine whether the spatial relationship between HFO and the SOZ changed as a function of sleep stage, Figure 6 shows the event rates from electrode contacts inside and

outside of the seizure onset zone (SOZ and nSOZ). The difference in ripple rates in SOZ and nSOZ contacts was highly significant in stages W, N1-N2, and N3 ($p < 0.000001$), but not in stage R ($p = 0.052$). Similarly, for fast ripples, the difference between rates in SOZ and nSOZ contacts was highly significant for stages N1-N2 and N3 ($p < 0.000001$), marginally significant for W ($p = 0.018$), and nonsignificant for stage R ($p = 0.90$). For spikes, the difference between SOZ and nSOZ contacts was highly significant in all stages ($p < 0.000001$), except for R ($p = 0.14$). For all event types, the rates were highest in N1-N2 and N3 sleep, independent of whether the contacts were in the SOZ.

Discussion

This study investigated the effect of sleep stage on the occurrence and properties of HFOs that were recorded using depth macroelectrodes in patients with focal epilepsy. Previous work in both humans and animal models has demonstrated the usefulness and selectivity of HFO, particularly above 250 Hz, as a method of defining the epileptogenic zone (Bragin et al., 1999b; Staba et al., 2002; Engel et al., 2003; Urrestarazu et al., 2007; Worrell et al., 2008). It, therefore, seems clear that incorporating the acquisition of SEEG data with a sufficiently high sampling rate to allow for the analysis of HFOs could have clinical benefits. However, before an investigation of HFOs can be reliably used in the clinical setting, more specific information needs to be acquired about how they vary as a function of the patient's state of consciousness. Progress has been made in this direction using recordings from microwires (Staba et al., 2004) but, as discussed in the Introduction, conclusions drawn from microelectrode studies cannot be directly transferred to macroelectrode recordings because of the very different size of the sampled neuronal populations (Jirsch et al., 2006; Jacobs et al., 2008). In a recent study, Worrell et al. (2008) explicitly examined the relationship between HFOs recorded with microelectrodes and macroelectrodes by using both types of recording contact in the same patients. They concluded that the local field potentials recorded by the different types of electrodes are qualitatively different, particularly with regard to the frequency of the observed events, with microwire recordings demonstrating a wider range of HFO frequencies. Given these observed differences, characterization of HFOs with explicit regard to the type of recording electrode is crucial.

There were two main purposes of this study. The first purpose was to determine whether non-REM sleep is associated with maximal rates of HFOs, in accordance with previous work in humans using depth microelectrodes (Staba et al., 2004), and more recently foramen ovale electrodes (Clemens et al., 2007). From a clinical point of view this is an important question. Although the acquisition of SEEG data from macroelectrodes to allow recording of HFO requires a relatively straightforward change of hardware, analysis to identify HFOs can be extremely time-consuming, and efforts need to be made to ensure that the epochs for data analysis are those with the highest possible rates of HFO.

The results from the current study indicate that the rates of HFOs recorded with macroelectrodes were indeed maximal in non-REM sleep, but they suggest that accurate sleep staging to distinguish N1-N2 from N3 is not necessary, since fast ripple rates were not significantly different in N1-N2 and N3 sleep. This may render the application of external EOG and EMG electrodes unnecessary. Recording with foramen ovale electrodes at a

sampling rate of 512 Hz, Clemens et al. (2007) were able to examine ripple but not fast ripple rates as a function of sleep stage. They found the highest ripple rates in non-REM sleep, with a significantly higher rate in non-REM stage 2 compared to slow-wave sleep. In the current study the opposite effect was found for ripples: the ripple rate was significantly higher in N3 than N1-N2. (Note that Clemens et al. used the nomenclature of Rechtschaffen and Kales, according to which slow-wave sleep is stages 3 and 4.) Staba et al. (2004), using depth microelectrodes and sampling at a rate of 10 kHz, also found the highest rates of both ripples and fast ripples in non-REM sleep, but did not distinguish between stages within non-REM. From these and the current study, a consistent picture emerges despite the difference in data-acquisition protocol and type of electrode.

Several studies have noted that HFOs tend to be closely related to spikes (Engel et al., 2003; Urrestarazu et al., 2007; Jacobs et al., 2008), but it is not clear whether they have a common generating mechanism which, for example, might suggest that they would have maximal rates of occurrence in the same stage of sleep. The data in this study showed that the majority of patients had a maximal spike rate in either N1-N2 or N3 sleep, and a consistent result was that the stage with the highest spike rate also had the highest rate of fast ripples. Two patients had spike rates in wakefulness that were comparable to those recorded in N1-N2 or N3 sleep (see Fig. 2). In patient 6, spike rates were similar in stages W, N1-N2, and N3, whereas both the ripple and fast ripple rates were clearly higher in stage N1-N2. Patient 7 had similarly high spike rates in stages W and N1-N2, with ripple rates also similar in these two stages. The rate of fast ripples was very low in this patient, but also highest in these stages. From these limited data it is, therefore, unclear how closely HFO rates follow spike rates or whether both are dependent purely on sleep stage. It would be interesting to examine this point further, since if spike rate could be used as a marker of HFO rate, the identification of the stage with maximal HFO rate would be made considerably easier. One thing that is clear from the current data and earlier studies is that both spikes and HFOs tend to be facilitated by slow-wave sleep, which differentiates them from seizures (Billiard et al., 1987).

The second main purpose of the study was to determine whether the properties of the HFOs detected in different sleep stages were consistent. Focusing on the stage with the highest HFO rates is only valid if the same amount of clinically relevant information is available from the observed events, that is, if the events identified in different sleep stages represent the same neurophysiological processes.

The results presented in this study show some significant differences between the HFO properties detected in the different stages of sleep. For example, ripple durations were significantly longer in stage N3 than in any other stage, whereas fast ripple durations were also longer in N3 than N1-N2. Although significant, the differences that were noted in HFO duration (Fig. 3), overlap with spikes (Fig. 4), and rates inside and outside of spikes were not dramatic (Fig. 5), with consistent values across all stages.

Perhaps the most important property from a clinical point of view is the extent to which HFOs distinguish between SOZ and nSOZ contacts. From this standpoint, it seems to be important to examine non-REM sleep (stages N1-N2 and N3), since the difference in rates

between SOZ and nSOZ contacts in REM sleep (stage R) was not significant for either ripples or fast ripples. Similarly, the difference in rates between SOZ and nSOZ contacts in wakefulness was marginally significant. Because the primary clinical use of HFO would be to obtain improved delineation of the SOZ, exclusion of wakefulness and REM sleep from the analysis may be important to maximize the distinction between SOZ and nSOZ. That said, this effect would be reduced as a result of the low rates of HFO in both stages if all stages were equally represented in the analysis section: although within stages W and R the spatial specificity of HFO is not as clear as in other stages, few events from these stages would contribute to the overall analysis. It has been suggested previously that REM sleep provides more clinically reliable information than other stages by demonstrating more restricted epileptic foci (Sammaritano et al., 1991). However, this conclusion was drawn from examination of interictal epileptiform discharges recorded on scalp EEG, events very different from those of the current study. The issue of the relationship between the neurophysiological generators of spikes and HFOs remains to a large extent open, but it is clear that it is potentially complex and requires further investigation.

One limitation of the current study was the lack of scalp electrodes to allow sleep staging according to all of the criteria of the AASM manual (Iber et al., 2007). This limits the extent to which all of the sleep stages can be distinguished, particularly the identification of stages N1 and N2, which requires observation of vertex sharp waves, K-complexes, and sleep spindles from scalp EEG. It was for this reason that the current study collapsed the results across stages N1 and N2, with stage N1-N2 being defined as non-REM, non–slow-wave sleep. As discussed in the Methods section, the majority of the sleep staging was done without explicit characterization of the SEEG activity, since the AASM manual does not refer to intracranial recordings. Despite this, the sleep staging was unambiguous in most cases. For example, wakefulness is easily recognized by the observation of blinking and muscle activity and REM sleep by EOG activity with quiescent EMG. High delta activity on intracranial EEG has been used as an indicator of slow-wave sleep in previous studies (Urrestarazu et al., 2007; Jacobs et al., 2008), and has been shown to be a hallmark of slow-wave sleep in intracranial recordings from the cat (Destexhe et al., 1999). This, and the remarkable consistency in the results across patients in terms of rates of spikes and HFOs (see Fig. 2), suggest that the same stages of sleep have been identified despite the lack of scalp electrodes.

Overall the analysis presented here suggests that sleep stage is unlikely to affect the neurophysiological mechanisms generating the HFOs, and affects only the rate with which consistent events occur. Accurate sleep staging to distinguish between stages N1-N2 and N3 is not necessary, since rates of HFO were similar. The occurrence of HFOs reliably distinguished between SOZ and nSOZ contacts, although in wakefulness and REM sleep this spatial specificity was diminished, indicating that exclusion of these stages from the analysis is desirable. When using depth macroelectrodes, analysis of fast ripples during non-REM sleep appears to be the best way of identifying the contacts in the SOZ.

Acknowledgments

This work was supported by the Wellcome Trust Value in People Awards Scheme and grant MOP-10189 from the Canadian Institutes of Health Research.

References

Billiard, M., Besset, A., Zachariev, Z., Touchon, J., Baldy-Moulinier, M., Cadilhac, J. Relation of seizures and seizure discharges to sleep stages. In: Wolf, P.Dam, M.Janz, D., Dreifuss, FE., editors. Advances in epileptology. Vol. 16. Raven Press; New York: 1987. p. 665-670.

Bragin A, Engel J Jr, Wilson CL, Fried I, Buzsáki G. High-frequency oscillations in human brain. Hippocampus. 1999a; 9:137–142. [PubMed: 10226774]

Bragin A, Engel J Jr, Wilson CL, Fried I, Mathern GW. Hippocampal and entorhinal cortex high-frequency oscillations (100–500 Hz) in human epileptic brain and in kainic acid-treated rats with chronic seizures. Epilepsia. 1999b; 40:127–137. [PubMed: 9952257]

Bragin A, Wilson CL, Staba RJ, Reddick M, Fried I, Engel J Jr. Interictal high-frequency oscillations (80–500 Hz) in the human epileptic brain: entorhinal cortex. Ann Neurol. 2002; 52:407–415. [PubMed: 12325068]

Clemens Z, Mçlle M, Erçss L, Barsi P, Halász P, Born J. Temporal coupling of parahippocampal ripples, sleep spindles and slow oscillations in humans. Brain. 2007; 130:2868–2878. [PubMed: 17615093]

Destexhe A, Contreras D, Steriade M. Spatiotemporal analysis of local field potentials and unit discharges in cat cerebral cortex during natural wake and sleep states. J Neurosci. 1999; 19:4595–4608. [PubMed: 10341257]

Draguhn A, Traub RD, Bibbig A, Schmitz D. Ripple (~200 Hz) oscillations in temporal structures. J Clin Neurophysiol. 2000; 17(4):361–376. [PubMed: 11012040]

Engel J Jr, Wilson C, Bragin A. Advances in understanding the process of epileptogenesis based on patient material: what can the patient tell us? Epilepsia. 2003; 44(Suppl 12):60–71. [PubMed: 14641562]

Gigli GL, Valente M. Sleep and EEG interictal epileptiform abnormalities in partial epilepsy. Clin Neurophysiol. 2000; 111(Suppl 2):S60–S64. [PubMed: 10996556]

Iber, C., Ancoli-Israel, S., Chesson, AL., Quan, SF. Rules, terminology and technical specifications. American Association of Sleep Medicine; Westchester, IL: 2007. The AASM manual for the scoring of sleep and associated events.

Jacobs J, LeVan P, Chander R, Hall J, Dubeau F, Gotman J. Interictal high-frequency oscillations (80–500 Hz) are an indicator of seizure onset areas independent of spikes in human epileptic brain. Epilepsia. 2008 May.9:2008. Epub ahead of print.

Jirsch JD, Urrestarazu E, LeVan P, Olivier A, Dubeau F, Gotman J. High-frequency oscillations during human focal seizures. Brain. 2006; 129:1593–1608. [PubMed: 16632553]

Sammaritano M, Gigli GL, Gotman J. Interictal spiking during wakefulness and sleep and the localization of foci in temporal lobe epilepsy. Neurology. 1991; 41:290–297. [PubMed: 1992379]

Staba RJ, Wilson CL, Bragin A, Fried I, Engel J Jr. Quantitative analysis of high frequency oscillations recorded in human epileptic hippocampus and entorhinal cortex. J Neurophysiol. 2002; 88:1743–1752. [PubMed: 12364503]

Staba RJ, Wilson CL, Bragin A, Jhung D, Fried I, Engel J Jr. High-frequency oscillations recorded in human medial temporal lobe during sleep. Ann Neurol. 2004; 56:108–115. [PubMed: 15236407]

Staba RJ, Frighetto L, Behnke EJ, Mathern GW, Fields T, Bragin A, Ogren J, Fried I, Wilson CL, Engel J Jr. Increased fast ripple to ripple ratios correlate with reduced hippocampal volumes and neuron loss in temporal lobe epilepsy patients. Epilepsia. 2007; 48:2130–2138. [PubMed: 17662059]

Urrestarazu E, Jirsch JD, LeVan P, Hall J, Dubeau F, Gotman J. High-frequency intracerebral EEG activity (100–599 Hz) following interictal spikes. Epilepsia. 2006; 47:1465–1476. [PubMed: 16981862]

Urrestarazu E, Chander R, Dubeau F, Gotman J. Interictal high-frequency oscillations (100–500 Hz) in the intracerebral EEG of epileptic patients. Brain. 2007; 130:2354–2366. [PubMed: 17626037]

Worrell GA, Parish L, Cranstoun SD, Jonas R, Baltuch G, Litt B. High-frequency oscillations and seizure generation in neocortical epilepsy. Brain. 2004; 127:1496–1506. [PubMed: 15155522]

Worrell GA, Gardner AB, Stead MS, Hu S, Goerss S, Cascino GJ, Meyer FB, Marsh R, Litt B. High-frequency oscillations in human temporal lobe: simultaneous microwire and clinical macroelectrode recordings. Brain. 2008; 131:928–937. [PubMed: 18263625]

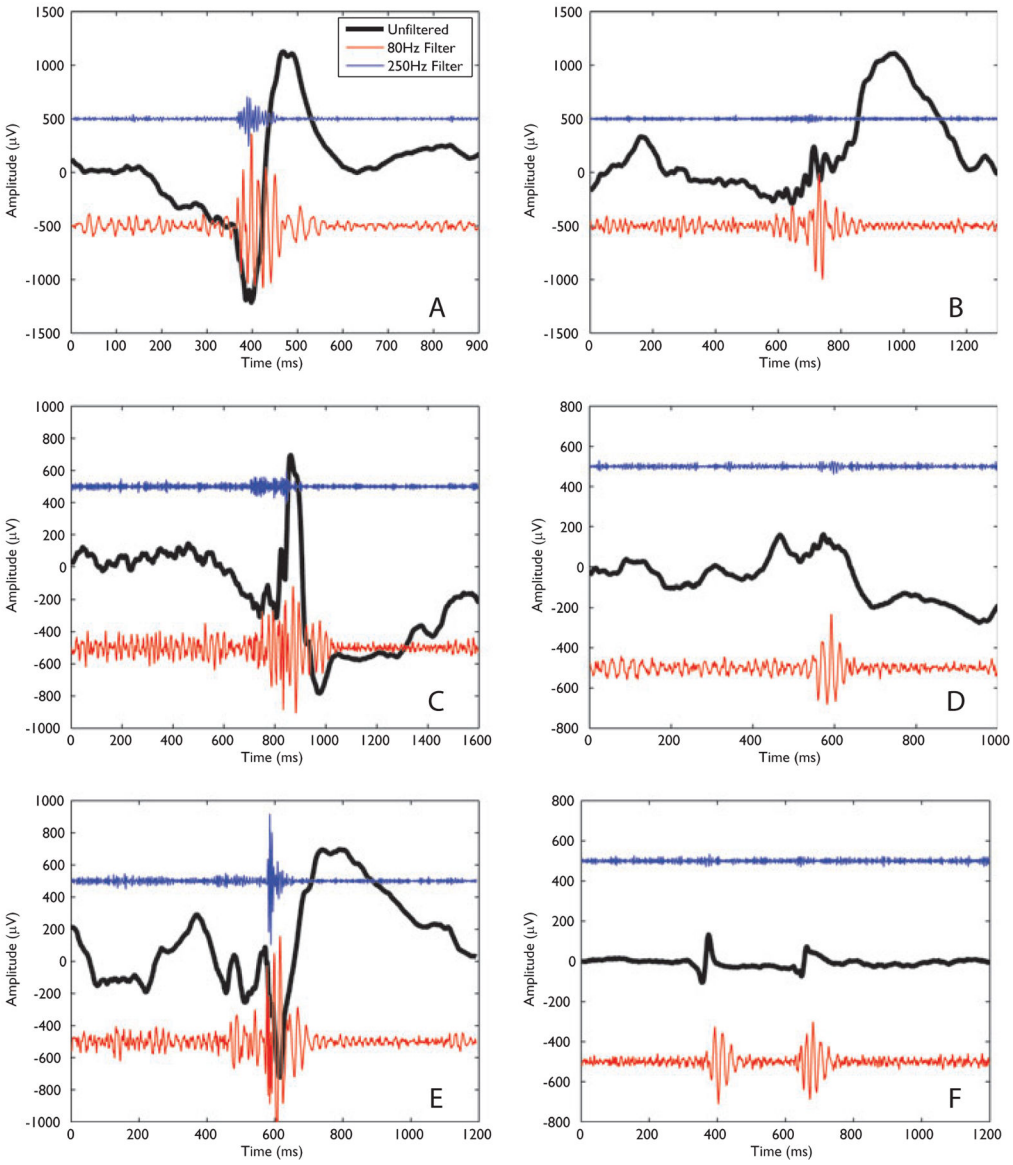

Figure 1.

Examples of ripples and fast ripples across patients and sleep stages. In each case the black trace shows the unfiltered data, whereas the lower (red) trace shows the ripple activity (80- Hz high-pass filter) and the upper (blue) trace shows the fast ripple activity (250- Hz high-pass filter). The amplitudes are as recorded, with the ripple and fast ripple activity having been multiplied by a factor of 10 to aid comparison. In addition, a constant offset has been added to separate the traces (the value of the constant was −500 μV for the ripple activity and 500 μV for the fast ripple activity). (**A**) Ripple and fast ripple from patient 1, contact RH1-RH2, sleep stage N3. (**B**) As for (**A**), but showing a ripple in the absence of a fast ripple. (**C**) Ripple and fast ripple identified in patient 5, contact LH1-LH2, stage N1-N2. (**D**) Data from patient 8, contact RH2-RH3, stage N3. A ripple was marked. (**E**) Ripple and fast ripple from patient 9, contact RA1-RA2, stage N1-N2. (**F**) Ripple in the absence of a fast ripple from patient 9, contact RAN2-RAN3, stage R.

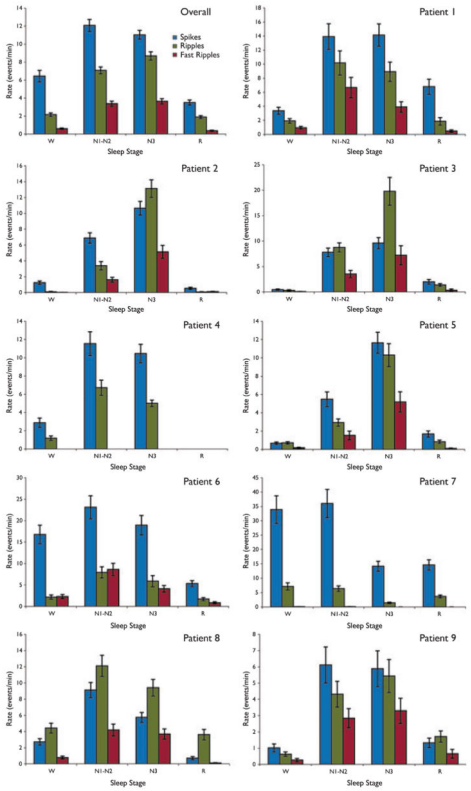

Figure 2.

Rates of spikes, ripples, and fast ripples in each sleep stage. The top left panel shows the mean rates over all subjects, whereas the other panels show the results for individual patients. In the majority of cases, rates of high-frequency oscillations (HFOs) were highest in either N1-N2 or N3 sleep. Results are plotted as the mean ± SEM.

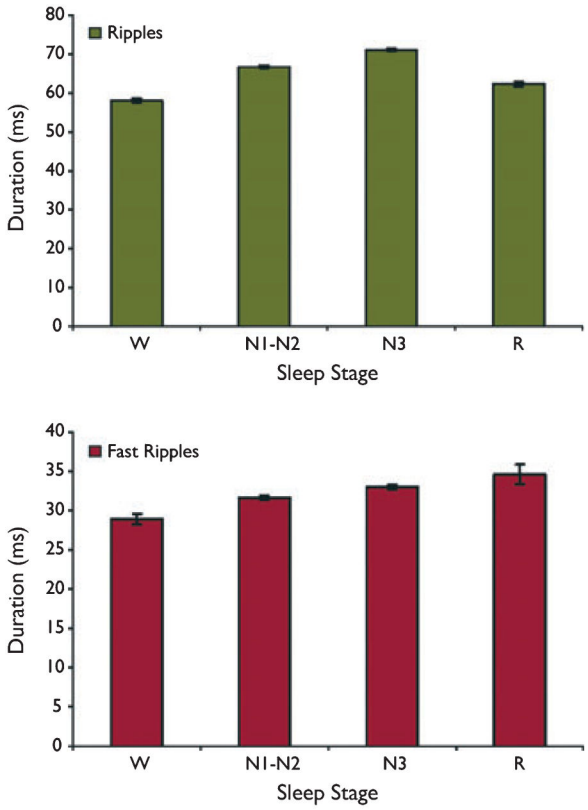

Figure 3.

Duration of ripple and fast ripple events as a function of sleep stage. Most of the paired comparisons were significant, although absolute differences in durations across sleep stage were small, with fast ripples in particular having a consistent duration. Results are plotted as the mean ± SEM.

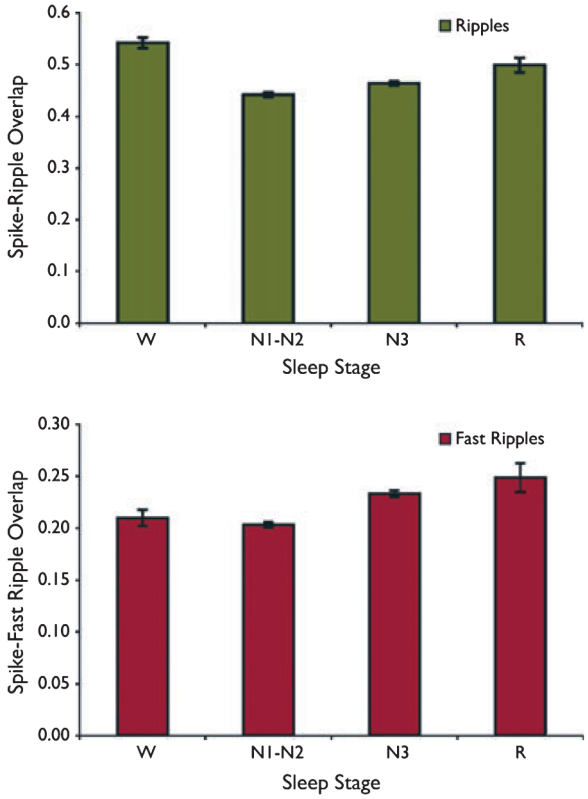

Figure 4.

Overlap between spikes and high-frequency oscillations (HFOs) as a function of sleep stage. The values observed for different sleep stages were consistent, with a similar proportion of HFOs occurring at the same time as spikes. Results are plotted as the mean ± SEM.

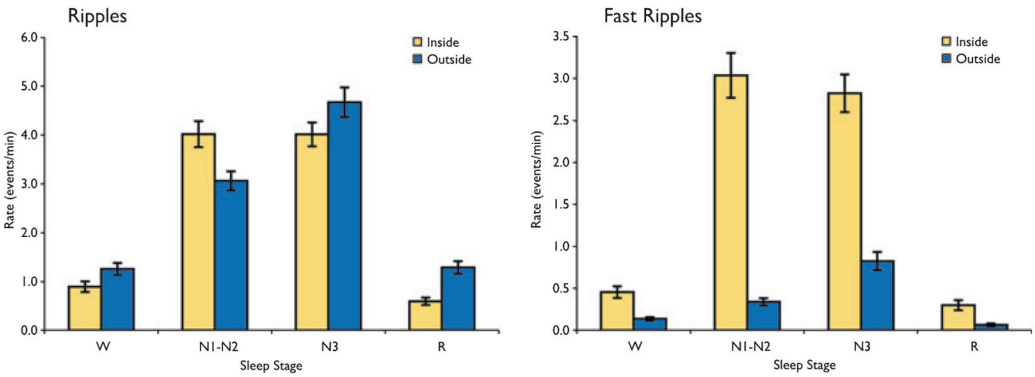

Figure 5.

The rates of high-frequency oscillations (HFOs) that occurred inside and outside of spike events. A similar pattern was observed for both as a function of sleep stage, with maximal rates in N1-N2 or N3 sleep. Results are plotted as the mean ± SEM.

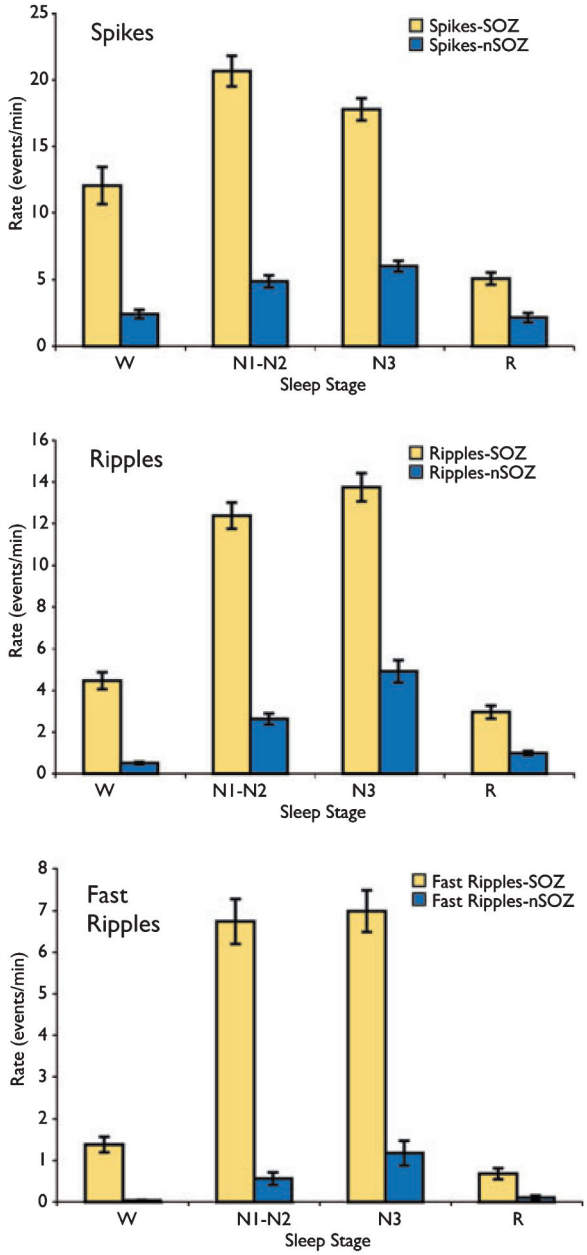

Figure 6.

Spatial specificity of high-frequency oscillations (HFOs) as a function of sleep stage. Rates of spikes and HFOs were considerably higher in seizure-onset zone (SOZ) electrodes, and this effect was largely maintained across sleep stages. Results are plotted as the mean ± SEM.

Epilepsia. Author manuscript; available in PMC 2013 October 07.

Table 1

Clinical data and implantation sites. In patients with temporal lobe epilepsy, a standard implantation consisting of three electrodes implanted orthogonally and pointing at the amygdala (A), hippocampus (HC), and the posterior hippocampus (PHC) was used

Patient number	Age/gender	Seizure semiology	Scalp EEG	MRI	Number of implanted electrodes	SEEG implantation sites	Analyzed contacts[a]
1	49/Fe	CPS, epigastric aura, cloni of the left face and arm	Ictal: bi T Interictal: L T	R MTL atrophy	6	L-HC, L-PHC, L-A R-HC, R-PHC, R-A Epidural L first T gyrus	LA6-LA7, LH4-LH5, LP2-LP3^{SOZ}, RA1-RA2, RA5-RA6, RH1-RH2^{SOZ}, RP1-RP2^{SOZ}
2	46/M	CPS, LOC, oral automatisms, agitation	Ictal: bi T Interictal: bi T	Malrotation R HC	4	L-HC, L-A, R-HC, R-A Epidural L and R first T gyrus	LA1-LA2, RA1-RA2^{SOZ}, RH1-RH2^{SOZ}, LH1-LH2, RH2-RH3^{SOZ}, RH3-RH4^{SOZ}, LH3-LH4, RA3-RA4
3	45/M	CPS, orofacial automatisms, bilateral hand movements	Ictal: L T Interictal: L T	L T pole atrophy	5	L-HC, L-PHC, L-A, L-OF, L T pole, Epidural L first T gyrus	LS1-LS2, LS2-LS3, LA1-LA2^{SOZ}, LH1-LH2^{SOZ}, LH3-LH4, LO1-LO2, LP6-LP7, LP1-LP2
4	33/M	CPS, laughter, bilateral hand automatisms, shaking of the head	Ictal: bi T Interictal: bi T	Tuberous sclerosis complex: 4 tuber	8	L-A, L-HC, L-OF, L-AC R-A, R-HC, R-OF, R-AC	LO1-LO2^{SOZ}, LO3-LO4^{SOZ}, LH1-LH2, RH2-RH3, RO1-RO2, LA1-LA2, RC3-RC4, RC6-RC7
5	44/M	CPS, automatisms, posturing of the right arm	Ictal: LT Interictal: bi T	L MTL atrophy	6	L-HC, L-PHC, L-A R-HC, R-PHC, R-A	LH4-LH5, RA1-RA2, LH1-LH2^{SOZ}, RH2-RH3, LP1-LP2, RP2-RP3, LA1-LA2^{SOZ}
6	54/Fe	CPS, epigastric aura, left hand numbness, LOC,	Ictal: R T Interictal: R T	R MTL atrophy R temporal-occipital posttraumatic contusion	5	R-HC, R-PHC, R-A, R-posterior-temporal junction in Le, R anterior occipital in Le Epidural E: first T, angular and supramarginal gyrus	RP1-RP2^{SOZ}, RH1-RH2^{SOZ}, RA1-RA2^{SOZ}, RH5-RH6, RC3-RC4, RP3-RP4, RO1-RO2, RO3-RO4
7	28/Fe	CPS, hypermotor seizures with urinary incontinence, mostly during sleep	Ictal: R F & T Interictal: bi F & T	FCD R F basal region and anterior insular cortex	7	L-AC, L-PC, L-OF R-AC, R-PC, R-OF, R-L (lesional through superior F gyrus aiming at the anterior insular)	LCP6-LCP7, LFO1-LFO2, RCA6-RCA7, RCP4-RCP5, RFO6-RFO7^{SOZ}, RFO7-RFO8^{SOZ}, RL3-RL4, RL5-RL6
8	25/M	CPS, LOC, manual and oral automatisms	Ictal: bi T Interictal: bi T	Bilateral periventricular Het.	9	L-HC, L-A, L-O (occipital lobe within Het), L-S (L trigone and supramarginal gyrus within Het) R-HC, R-PHC, R-A, R-O (R occipital within Het), R-S (R trigonal area and supramarginal gyrus within Het)	LH2-LH3^{SOZ}, RH2-RH3^{SOZ}, RH1-RH2^{SOZ}, RA1-RA2^{SOZ}, RS3-RS4, RO1-RO2, RP1-RP2, LH1-LH2^{SOZ}, LA1-LA2^{SOZ}, LS1-LS2, LO1-LO2, RS1-RS2, LS4-LS5
9	24/M	CPS, LOC, automatisms, urinary incontinence	Ictal: R T Interictal: R T	Two nodular Het in the right trigonal area	5	R-HC, R-PHC, R-A, R-AN (Anterior Le R trigonal area), R-PN (posterior	RA1-RA2^{SOZ}, RH1-RH2^{SOZ}, RAN5-RAN6, RAN1-RAN2,

Patient number	Age/gender	Seizure semiology	Scalp EEG	MRI	Number of implanted electrodes	SEEG implantation sites	Analyzed contacts[a]
						Le R trigonal area). Epidural over first T and supramarginal gyrus	RAN2-RAN3, RPN1-RPN2, RPN2-RPN3

A, amygdala; AC, anterior cingulate; bi, bilateral; CPS, complex partial seizure; F, frontal; Fe, female; FCD, focal cortical dysplasia; HC, hippocampus; Het, heterotopia; L, left; LOC, loss of contact; M, male; MTL, mesial temporal lobe; OF, orbitofrontal; PC, posterior cingulate; PHC, posterior hippocampus; R, right; SMA, supplementary motor area; T, temporal.

[a]Superscript “SOZ” indicates that the contact was in the seizure-onset zone.